

Orbitally forced ice sheet fluctuations during the Marinoan Snowball Earth glaciation

Benn, Douglas I.; Le Hir, Guillaume; Bao, Huiming; Donnadieu, Yannick; Dumas, Christophe; Fleming, Edward J.; Hambrey, Michael J.; McMillan, Emily A.; Petronis, Michael S.; Ramstein, Gilles; Stevenson, Carl T. E.; Wynn, Peter M.; Fairchild, Ian J.

DOI:
[10.1038/ngeo2502](https://doi.org/10.1038/ngeo2502)

License:
None: All rights reserved

Document Version
Peer reviewed version

Citation for published version (Harvard):
Benn, DI, Le Hir, G, Bao, H, Donnadieu, Y, Dumas, C, Fleming, EJ, Hambrey, MJ, McMillan, EA, Petronis, MS, Ramstein, G, Stevenson, CTE, Wynn, PM & Fairchild, IJ 2015, 'Orbitally forced ice sheet fluctuations during the Marinoan Snowball Earth glaciation', *Nature Geoscience*, vol. 8, no. 9, pp. 704-707.
<https://doi.org/10.1038/ngeo2502>

[Link to publication on Research at Birmingham portal](#)

Publisher Rights Statement:

Final Version of Record published as: Benn, Douglas I., et al. "Orbitally forced ice sheet fluctuations during the Marinoan Snowball Earth glaciation." *Nature Geoscience* 8.9 (2015): 704-707. Available online: <http://dx.doi.org/10.1038/ngeo2502>

Checked October 2015

General rights

Unless a licence is specified above, all rights (including copyright and moral rights) in this document are retained by the authors and/or the copyright holders. The express permission of the copyright holder must be obtained for any use of this material other than for purposes permitted by law.

- Users may freely distribute the URL that is used to identify this publication.
- Users may download and/or print one copy of the publication from the University of Birmingham research portal for the purpose of private study or non-commercial research.
- User may use extracts from the document in line with the concept of 'fair dealing' under the Copyright, Designs and Patents Act 1988 (?)
- Users may not further distribute the material nor use it for the purposes of commercial gain.

Where a licence is displayed above, please note the terms and conditions of the licence govern your use of this document.

When citing, please reference the published version.

Take down policy

While the University of Birmingham exercises care and attention in making items available there are rare occasions when an item has been uploaded in error or has been deemed to be commercially or otherwise sensitive.

If you believe that this is the case for this document, please contact UBIRA@lists.bham.ac.uk providing details and we will remove access to the work immediately and investigate.

Orbitally Forced Ice Sheet Fluctuations in Snowball Earth

Douglas I. Benn,^{1,2*} Guillaume Le Hir,³ Huiming Bao,⁴ Yannick Donnadieu,⁵ Christophe Dumas,⁵ Edward J. Fleming,^{1,6,7} Michael J. Hambrey,⁸ Emily A. McMillan,⁶ Michael S. Petronis,⁹ Gilles Ramstein,⁵ Carl T.E. Stevenson,⁶ Peter M. Wynn,¹⁰ Ian J. Fairchild⁶

¹Department of Geology, The University Centre in Svalbard (UNIS), N-9171 Longyearbyen, Norway.

²School of Geography and Geosciences, University of St Andrews, St Andrews KY16 8YA, Scotland, UK.

³Institut de Physique du Globe de Paris, Paris, France

⁴Department of Geology and Geophysics, E235 Howe-Russell Complex, Louisiana State University, Baton Rouge, LA 70803, USA.

⁵Laboratoire des Sciences du Climat et de l'Environnement, CNRS-CEA, Gif-sur-Yvette, France

⁶School of Geography, Earth and Environmental Sciences, University of Birmingham B15 2TT, UK.

⁷Current address: CASP, West Building, 181A Huntingdon Road, Cambridge, CB3 0DH, UK

⁸Institute of Geography and Earth Sciences, Aberystwyth University, Aberystwyth, Wales, UK.

⁹Natural Resource Management, Environmental Geology,, New Mexico Highlands University, Las Vegas, New Mexico, USA.

¹⁰Lancaster Environment Centre, University of Lancaster, Lancaster LA1 4YQ, UK.

*Corresponding author. E-mail: Doug.Benn@unis.no

Snowball Earth theory provides a powerful framework for understanding Neoproterozoic panglaciations, although some of its predictions are apparently contradicted by geological evidence. For example, Snowball theory posits that the panglaciations were terminated after millions of years of fridity by a positive feedback, in which initial warming from rising atmospheric CO₂ was amplified by reduction of ice cover and planetary albedo (1, 2). This threshold behaviour implies that most of the glacial record was deposited in a brief 'melt-back' period (3), an interpretation apparently inconsistent with geological evidence for glacial-interglacial cycles in low palaeolatitudes (4-6). [Here we use geological and geochemical evidence combined with numerical modeling experiments to reconcile these apparently conflicting views. New evidence from Svalbard \(Norwegian High Arctic\) indicates oscillating glacier extent and hydrological conditions within continental deposits of a Cryogenian glaciation, during a period when pCO₂ was uniformly high. Modeling experiments show that such oscillations can be explained by orbital forcing in the late stages of a 'Snowball' glaciation, while pCO₂ was rising towards the threshold required for complete melt-back. \[This reconciles Snowball Earth theory with evidence for the complex successions observed at many other localities.\]\(#\)](#)

The Wilsonbreen Formation in NE Svalbard contains a detailed record of environmental change during the Marinoan, the second of the major Cryogenian glaciations (650-635 Ma) (7, 8). At this time, Svalbard was located in the Tropics on the eastern side of Rodinia (9, 10). The Wilsonbreen Formation is up to up to 180 m thick and was deposited within a long-lived intracratonic sedimentary basin (11). It is subdivided into three members (W1, W2 and W3) based on the relative abundance

of diamictite and carbonate beds (7, 8; Fig. 1; Supplementary Figures 1 & 2). The occurrence of lacustrine sediments containing both precipitated carbonate and ice-rafted detritus throughout the succession, and intermittent evaporative carbonates and fluvial deposits, indicates ~~deposition in a closed terrestrial basin. That the~~ basin remained isolated from the sea throughout deposition of the Wilsonbreen Formation, ~~consistent with due to~~ eustatic sea level fall of several hundred metres ~~during the Marinoan and limited local isostatic depression~~ (Supplementary Information; 12). This makes it an ideal location to investigate the possibility of climate cycles within a Neoproterozoic panglaciation, as it provides direct evidence of subaerial environments and climatic conditions.

We made detailed sedimentary logs at ten known and new localities extending over 60 km of strike (Fig. 1; Supplementary Figure 1; see Methods). Seven sediment facies associations were identified, recording distinct depositional environments that varied in spatial extent through time (Supplementary Figure 3; Supplementary Information). These are: FA1: *Subglacial*, recording direct presence of glacier ice, FA2: *Fluvial channels*, FA3: *Dolomitic floodplain*, recording episodic flooding, evaporation and microbial communities; FA4: *Carbonate lake margin*, including evidence of wave action; FA5: *Carbonate lacustrine*, including annual rhythmites and intermittent ice-rafted debris; FA6: *Glacilacustrine*, consisting of ice-proximal grounding-line fans (FA6-G) and ice-distal rainout deposits (FA6-D); and FA7: *Periglacial*, recording cold, non-glacial conditions. Additional descriptions are provided in the Supplementary Information. The vertical and horizontal distribution of these facies associations (Fig. 1) allows the sequence of environmental changes to be reconstructed in detail.

(1) The base of the Formation is a well-marked periglacially weathered horizon with thin wind-blown sands (Supplementary Figure 4a-b). This surface records very limited sediment cycling in cold, arid conditions.

(2) At all localities, the weathering horizon is overlain by fluvial channel facies (FA2) and mudstones, marking the appearance of flowing water in the basin and implying positive air temperatures for at least part of the time (Supplementary Figure 5a).

(3) Glacilacustrine deposits (FA6-D) record flooding of the basin and delivery of sediment by ice-rafting (Supplementary Figure 4c-d). Far-travelled clasts are common, indicating transport by a large, continental ice sheet.

(4) Warm-based, active ice advanced into the basin, indicated by traction tills and glacitectonic shearing (FA1; Supplementary Figure 4e-g).

(5) Ice retreat is recorded by a second periglacial weathering surface (FA7) developed on unconsolidated sediment at the top of member W1. This is overlain by fluvial channel, floodplain, lake-margin and carbonate lacustrine sediments of W2 (FA2-5; Supplementary Figure 5), recording a shifting mosaic of playa lakes and ephemeral streams. Lakes and river channels supported microbial communities. Millimetre-scale carbonate-siliciclastic rhythmites indicate seasonal cycles of photosynthesis. Overall, the environment appears to have been closely similar to that of the present-day McMurdo Dry Valleys in Antarctica, though with less extreme seasonality due to its low latitude (13).

(6) Water levels and glacier extent underwent a series of oscillations, recorded by switches between glacilacustrine diamictite (FA6-D) and fluvial, lacustrine and lake-margin sediments (FA2-5) in member W2. Sedimentation rates inferred from annual

rhythmites in member W2 suggest that each retreat phase may have lasted $\sim 10^4$ years.

(7) A second major ice advance marks the base of W3, with widespread deposition of subglacial tills and glaciectonism of underlying sediments. Basal tills are absent from the northernmost locality, but close proximity of glacier ice is recorded by grounding-line fans (FA6-G; Supplementary Figure 4h-i).

(8) Ice retreated while the basin remained flooded and glacial sediment continued to be delivered to the lake by ice rafting. Thin laminated carbonates (FA5) in W3 indicate periods of reduced glacial sedimentation, indicative of minor climatic fluctuations over timescales of $\sim 10^3$ years (Supplementary Figure 5g).

(9) A sharp contact with overlying laminated 'cap' carbonate (Supplementary Figure 2) records the transition to post-glacial conditions. At some localities, basal conglomerates provide evidence of subaerial exposure followed by marine transgression. The cap carbonate closely resembles basal Ediacaran carbonates elsewhere, and marks global deglaciation, eustatic sea-level rise and connection of the basin to the sea (1, 12, 14).

Environmental and atmospheric conditions during deposition of W2 and W3 can be further elucidated by isotopic data from carbonate-associated sulphate in lacustrine limestones (Fig. 2 and Supplementary Figure 6). These display negative to extremely negative $\Delta^{17}\text{O}$ values with consistent linear co-variation with $\delta^{34}\text{S}$, indicating mixing of pre-glacial sulphate and isotopically light sulphate formed in a CO_2 -enriched atmosphere (15, 16). The observed values could reflect non-unique combinations of $p\text{CO}_2$, $p\text{O}_2$, O_2 residence time and other factors, but a box model (17) indicates $p\text{CO}_2$ was most likely ~ 10 to 100 mbar (1 mbar = 1000 ppmv).

These values are too high to allow formation of low-latitude ice sheets in the Neoproterozoic, but they are consistent with a late-stage Snowball Earth. For an ice-free Neoproterozoic Earth, model studies indicate mean terrestrial temperatures in the range 30-50°C for $p\text{CO}_2 = 10$ to 100 mbar (18). Formation of low-latitude ice sheets requires much lower $p\text{CO}_2$, on the order of 0.1 - 1 mbar (2, 19, 20), but once formed, high albedo ice cover can maintain low planetary temperatures despite rising $p\text{CO}_2$. This hysteresis in the relationship between $p\text{CO}_2$ and planetary temperature is a key element of Snowball Earth theory. It implies that W2 and W3 were deposited relatively late in the Marinoan, after volcanic outgassing had raised $p\text{CO}_2$ from 0.1 or 1 mbar to 10 or 100 mbar. Modelled silicate weathering and volcanic outgassing rates indicate that this would require 10^6 to 10^7 years (21).

The consistent co-variation of $\Delta^{17}\text{O}$ and $\delta^{34}\text{S}$ in lacustrine limestones in both W2 and W3 suggests no detectable rise in atmospheric $p\text{CO}_2$, as this would alter the slope of the mixing line (Fig. 2). This implies that the glacier oscillations recorded in deposition of both W2 and W3 occurred in during a relatively short time interval ($<10^5$ years, 21). ~~We therefore infer that the glacier oscillations recorded in the Wilsonbreen Formation occurred during a relatively brief period toward the end of the Marinoan, whereas the much longer period during which~~ This implies a long hiatus in the geological record, while $p\text{CO}_2$ built up from the low values necessary to initiate low-latitude glaciation (0.1 or to 1 mbar) to those indicated by the geochemical evidence. may have been characterized by cold, arid conditions represented only by t The basal weathering horizon may record cold arid conditions during part of this interval.

The evidence for ice-sheet advance/retreat cycles at low latitudes in a CO₂-enriched atmosphere motivated a series of numerical simulations to test the hypothesis that these cycles were linked to Milankovitch orbital variations. We employed asynchronous coupling of a 3D ice sheet model and an Atmospheric General Circulation Model using the continental configuration of (22). We first ran simulations with a modern orbital configuration to examine ice-sheet behaviour through a large range of $p\text{CO}_2$ values from 0.1 to 100 mbar, as used in previous studies (23; Supplementary Figures 7-10). Consistently with previous results (2, 20), at low $p\text{CO}_2$ (0.1 mbar), global ice volume reaches $170 \times 10^6 \text{ km}^3$ but substantial tropical land areas remain ice free due to sublimation exceeding snowfall (Supplementary Figure S10a). Ice volume remains relatively constant for $p\text{CO}_2 = 0.1$ to 20 mbar (Supplementary Figure S10b), due to an increase in accumulation that compensates for higher ablation rates (Supplementary Figure 13). In contrast, above 20 mbar, ice extent in the eastern Tropics significantly decreases (Supplementary Figure 10c). At $p\text{CO}_2 = 100$ mbar, most of the continental ice cover disappears except for remnants over mountain ranges (Supplementary Figure 10d).

To test the sensitivity of the tropical ice sheets to Milankovitch forcing, experiments with changing orbital parameters were initialized using the steady-state ice sheets for $p\text{CO}_2 = 20$ mbar. Although obliquity has been invoked as a possible cause of Neoproterozoic glaciations (24), this mechanism remains problematical and cannot account for significant climatic oscillations at low latitudes (25, 26). We therefore focused on precession as a possible driver, and used two opposite orbital configurations favoring cold and warm summers, respectively, over the northern tropics (CSO: cold summer orbit and WSO: warm summer orbit) (Supplementary

Figure 14). Switching between these configurations causes tropical ice-sheets to advance/retreat over several hundred kilometers in 10 kyr (Supplementary Movie 1), with strong asymmetry between hemispheres (Fig. 3). Shifting from WSO to CSO causes ice retreat in the southern hemisphere, while ice sheet expansion occurs in the northern hemisphere (Supplementary Figure 14c-d). Significant ice volume changes occur between 30° N and S, but are less apparent in higher latitudes. This reflects higher ablation rates in the warmer low latitudes (Supplementary Figure 14e-h), and higher ice-sheet sensitivity to shifting patterns of melt. Larger greenhouse forcing at the end of the Snowball event implies increasing ice-sheet sensitivity to subtle insolation changes. Given a strong diurnal cycle (23), our simulations also predict a significant number of days above 0°C in the tropics (Supplementary Figure 15), consistent with geological evidence for ice rafting, liquid water in lakes and rivers, and photosynthetic microbial communities.

Our results show that geological evidence for glacial-interglacial cycles (5-7) is consistent with an enriched Snowball Earth theory. Termination of the Marinoan panglaciation was not a simple switch from icehouse to greenhouse states but was characterized by a climate transition during which glacial cycles could be forced by Milankovitch orbital variations. The geochemical evidence presented here implies that at least the upper 60-70% of the Wilsonbreen Formation was deposited in $\sim 10^5$ years, on the assumption that a trend in $p\text{CO}_2$ would be evident over longer timescales (21). Rates of CO_2 build-up, however, may have significantly slowed in the later stages of Snowball Earth due to silicate weathering of exposed land surfaces, so it is possible that the oscillatory phase was more prolonged.

~~The Initiation of low latitude glaciation in the Neoproterozoic requires low $p\text{CO}_2$~~

Formatted: Font: Italic

~~(0.1 - 1 mbar, 2, 19, 20), implying that the~~ oscillatory phase was preceded by a
prolonged period ($\sim 10^6$ to 10^7 years) during which $p\text{CO}_2$ gradually increased by
volcanic outgassing ~~(21) from the low levels (0.1 - 1 mbar) required for glacial~~
~~initiation. In the Wilsonbreen Formation, this period appears to be represented~~
~~solely by the basal weathering horizon, consistent with a 'deep Snowball' state with~~
~~low temperatures and a limited hydrological cycle.~~ This timescale is consistent with
recent dating evidence for the duration of Cryogenian glaciations (27).

Formatted: Subscript

Additional work is needed to refine the upper and lower limits of $p\text{CO}_2$ conducive
to climate and ice-sheet oscillations in Snowball Earth. Factors not included in the
present model, such as supraglacial dust or areas of ice-free tropical ocean (28-30),
can be expected to make the Earth system more sensitive to orbital forcing. While
many details remain to be investigated, our overall conclusions remain robust.

The Neoproterozoic Snowball Earth was nuanced, varied and rich. We anticipate
that detailed studies of the rock record in other parts of the world, in conjunction
with numerical modeling studies, will continue to yield insight into the temporal and
regional diversity of this pivotal period in Earth history.

Methods

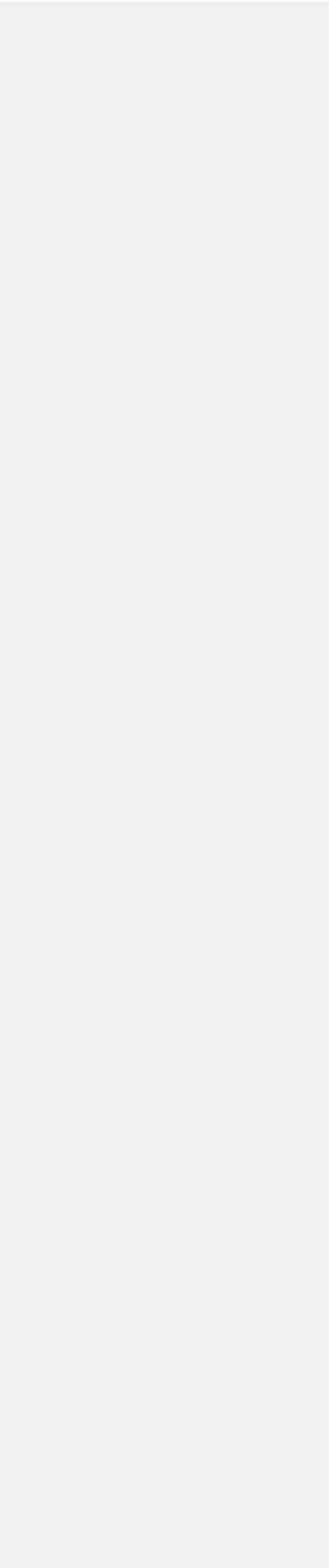
Sedimentology. Lithofacies were classified based on grain size, internal sedimentary
structures and deformation structures, and bounding surfaces. Detailed stratigraphic
logs were made in the field, supplemented by drawings and photographs of key

features. Samples were taken for polishing and thin sectioning, to allow detailed examination of microstructures in the laboratory. In addition, data were collected on clast lithology, shape, surface features and fabric. Diamictites of the Wilsonbreen Formation are commonly very friable, allowing included clasts to be removed intact from the surrounding matrix, allowing measurement of both clast morphology and orientation, using methods developed for unlithified sediments. Clast morphology (shape, roundness and surface texture) was measured for samples of 50 clasts to determine transport pathways. Clast fabric analysis was performed by measuring α -axis orientations of samples of 50 clasts with a compass-clinometer, and data were summarized using the eigenvalue or orientation tensor method. Orientated samples for measurement of Anisotropy of Magnetic Susceptibility (AMS) were collected using a combination of field-drilling and block sampling. AMS was measured using an AGICO KLY-3 Kappabridge operating at 875 Hz with a 300 A/m applied field at the University of Birmingham and an AGICO MFK-1A Kappabridge operating at 976 Hz with a 200 A/m applied field at New Mexico Highlands University.

Geochemistry. Laboratory procedures for extracting, purifying, and measuring the triple oxygen ($\delta^{18}\text{O}$ and $\Delta^{17}\text{O}$) and sulfur ($\delta^{34}\text{S}$) isotope composition of CAS in bulk carbonates are detailed in ref 16. Briefly, fresh carbonate-bearing rock chips were crushed into fine grains and powders using mortar and pestle. Rinsing the fines with 18 M Ω water revealed little water-leachable sulphate in all the Wilsonbreen carbonates. Subsequently, ca. 10 to 30 g carbonates were slowly digested in 1-3 M HCl solutions. The solution was then centrifuged, filtered through a 0.2 μm filter, and acidified before saturated BaCl_2 droplets were added. BaSO_4 precipitates were

collected after >12 hours and purified using the DDARP method (see Supporting Information). The purified BaSO₄ was then analyzed for three different isotope parameters: 1) $\Delta^{17}\text{O}$, by converting to O₂ using a CO₂-laser fluorination method; 2) $\delta^{18}\text{O}$, by converting to CO through a Thermal Conversion Elemental Analyzer (TCEA) at 1450 °C; and 3) $\delta^{34}\text{S}$, by converting to SO₂ by combustion in tin capsules in the presence of V₂O₅ through an Elementar Pyrocube elemental analyzer at 1050 °C. The $\Delta^{17}\text{O}$ was run in dual-inlet mode while the $\delta^{18}\text{O}$ and $\delta^{34}\text{S}$ in continuous-flow mode. Both the $\Delta^{17}\text{O}$ and $\delta^{18}\text{O}$ were run on a MAT 253 at Louisiana State University whilst the $\delta^{34}\text{S}$ was determined on an Isoprime 100 continuous flow mass spectrometer at the University of Lancaster, UK. The $\Delta^{17}\text{O}$ was calculated as $\Delta^{17}\text{O} \equiv \delta'^{17}\text{O} - 0.52 \times \delta'^{18}\text{O}$ in which $\delta' \equiv 1000 \ln (R_{\text{sample}}/R_{\text{standard}})$ and R is the molar ratio of ¹⁸O/¹⁶O or ¹⁷O/¹⁶O. All δ values are in VSMOW and VCDT for sulphate oxygen and sulfur respectively. The analytical standard deviation (1 σ) for replicate analysis associated with the $\Delta^{17}\text{O}$, $\delta^{18}\text{O}$, and $\delta^{34}\text{S}$ are $\pm 0.05\text{‰}$, $\pm 0.5\text{‰}$, and $\pm 0.2\text{‰}$, respectively. Since the CAS is heterogeneous in hand-specimen, the standard deviation is for laboratory procedures. $\delta^{34}\text{S}$ values were corrected against VCDT using within run analyses of international standard NBS-127 (assuming $\delta^{34}\text{S}$ values of +21.1 ‰). Within-run standard replication (1 SD) was <0.3 ‰. All geochemical data are included in Supplementary Table 1.

Details of the numerical modelling are provided in the Supplementary Information in the online version of the paper. Code for the GCM LMDz is freely available at: <http://lmdz.lmd.jussieu.fr> but the ISM GRISLI (GRenoble Ice Shelf and Land Ice model) is in limited access.



References

- (1) Hoffman, P.F. and Schrag, D.P. The Snowball Earth hypothesis: testing the limits of global change. *Terra Nova* **14**, 129-155 (2002).
- (2) Donnadieu, Y., Godd  ris, Y. and Le Hir, G. Neoproterozoic atmospheres and glaciation. In: *Treatise on Geochemistry*, Second Edition Vol. 6, 217-229 (2014).
- (3) Hoffman, P.F. Strange bedfellows: glacial diamictite and cap carbonate from the Marinoan (635Ma) glaciation in Namibia. *Sedimentology* **58**, 57-119 (2011).
- (4) Allen, P.A. and Etienne, J.L. Sedimentary challenge to Snowball Earth. *Nat Geosci* **1**, 817-825 (2008).
- (5) Rieu, R., Allen, P.A., Pl  tze, M. and Pettke, T. Climatic cycles during a Neoproterozoic 'snowball' glacial epoch. *Geology* **35**, 299-302 (2007).
- (6) Le Heron, D.P., Busfield, M.E., and Kamona, F. An interglacial on snowball Earth? Dynamic ice behaviour revealed in the Chuos Formation, Namibia. *Sedimentology* **60**, 411-427 (2013).
- (7) Fairchild, I.J. and Hambrey, M.J. Vendian basin evolution in East Greenland and NE Svalbard. *Precambrian Res* **73**, 217–233 (1995).
- (8) Halverson, G.P. A Neoproterozoic Chronology IN: Xiao, S. & Kaufman, A.J. (Eds.) *Neoproterozoic Geobiology and Paleobiology*, 231-271 (Springer, New York, 2006).
- (9) Li, X.-X., Evans, D.A. and Halverson, G.P. Neoproterozoic glaciations in a revised global palaeogeography from the breakup of Rodinia to the assembly of Gondwanaland. *Sediment Geol* **294**, 219-232 (2013).

(10) Petronis, M S, Stevenson, C, Fleming, E J, Fairchild, I J, Hambrey, M, Benn, D I., 2013, Paleomagnetic Data from the Neoproterozoic Wilsonbreen Formation, Ny Friesland, Svalbard, Norway and Preliminary Data from the Storeelv Formation, Ella Ø, Kong Oscar Fjord, East Greenland, American Geophysical Union, Fall Meeting 2013, abstract #GP41A-1107.

(11) Harland, W.B. *The Geology of Svalbard*. Geol. Soc. London Mem., 17 (Geological Society, London, 1997).

(12) Creveling, J.R. and Mitrovica, J.X. The sea-level fingerprint of a Snowball Earth deglaciation. *Earth Planet Sc Lett* **399**, 74–85 (2014).

(13) Lyons, W.B. et al. The McMurdo Dry Valleys long-term ecological research program: new understanding of the biogeochemistry of the Dry Valley lakes: a review. *Polar Geography* **25**, 202-217 (2001).

(14) Hoffman, P. et al. Are basal Ediacaran (635 Ma) basal 'cap dolostones' diachronous? *Earth Planet Sc Lett* **258**, 114-131 (2007).

(15) Fairchild, I.J., Hambrey, M.J., Spiro, B. and Jefferson, T.H. Late Proterozoic glacial carbonates in northeast Spitsbergen: new insights into the carbonate-tillite association. *Geol Mag* **126**, 469-490 (1989).

(16) Bao, H., Fairchild, I.J., Wynn, P.M. and Spötl, C. Stretching the envelope of past surface environments: Neoproterozoic glacial lakes from Svalbard. *Science* **323**,119-122 (2009).

(17) Cao, X. and Bao, H. Dynamic model constraints on oxygen-17 depletion in atmospheric O₂ after a Snowball Earth. *P Natl Acad Sci USA* **110**, 14546–14550 (2013).

- (18) Le Hir, G. et al. The snowball Earth aftermath: Exploring the limits of continental weathering processes. *Earth Planet Sc Lett* **277**, 453–463 (2009).
- (19) Pierrehumbert, R., Abbot, D.S., Voigt, A. and Koll, D. Climate of the Neoproterozoic. *Ann Rev Earth Planet Sci* **39**, 417-460 (2011).
- (20) Pollard, D. and Kasting, J.F. Climate-ice simulations of Neoproterozoic glaciation before and after collapse to Snowball Earth. In: G.S. Jenkins, M.A.S. McMenamin, C.P. McKay and L. Sohl (eds.) *The Extreme Proterozoic: Geology, Geochemistry, and Climate*. Geophys. Monogr. Ser. 146 (AGU, Washington, D.C. 2004).
- (21) Le Hir, G., Ramstein, G., Donnadiieu, Y. and Godd  ris, Y. Scenario for the evolution of atmospheric pCO₂ during a snowball Earth. *Geology* **36**, 47–50 (2008).
- (22) Hoffman, P.F., Li, Z.X., A palaeogeographic context for Neoproterozoic glaciation. *Palaeogeogr Palaeocl* **277**, 158–172 (2009).
- (23) Pierrehumbert, R.T. Climate dynamics of a hard Snowball Earth. *J Geophys Res* **110**, DOI: 10.1029/2004JD005162 (2005).
- (24) Spiegl, T. C., Paeth, H. and Frimmel, H.E., Evaluating key parameters for the initiation of a Neoproterozoic Snowball Earth with a single Earth System Model of intermediate complexity. *Earth Planet Sc Lett* **415**, 100-110 (2015).
- (25) Donnadiieu, Y., Ramstein, G., Fluteau, F., Besse, J. and Meert, J. Is high obliquity a plausible cause for Neoproterozoic glaciations? *Geophys Res Lett* **29**, DOI: 10.1029/2002GL015902 (2002).
- (26) Paillard, D. Quaternary glaciations: from observations to theories. *Quaternary Sci Rev* **107**, 11-24 (2015).

(27) Rooney, A.D. et al. ~~Re-Os geochronology and coupled Os-Sr isotope constraints on the Sturtian snowball Earth. *PNAS* **111**, doi: 10.1073/pnas.1317266110~~ A Cryogenican chronology: Two long-lasting synchronous Neoproterozoic glaciations. *Geology* **43**, 459-462 (20152014).

(28) Abbot, D.S. and Pierrehumbert, R.T. Mudball: surface dust and Snowball Earth deglaciation. *J Geophys Res* **115**, DOI: 10.1029/2009JD012007 (2010).

(29) Abbot, D.S., Voigt, S. and Koll, D. The Jormungand global climate state and implications for Neoproterozoic glaciations. *J Geophys Res-Atmos* **116**, DOI: 10.1029/2011JD015927 (2011).

(30) Rose, B. E. J. Stable “Waterbelt” climates controlled by tropical ocean heat transport: A nonlinear coupled climate mechanism of relevance to Snowball Earth. *J Geophys Res-Atmos* **120**, doi:10.1002/2014JD022659 (2015).

Correspondence and requests for materials should be addressed to Doug Benn (doug.benn@unis.no).

Acknowledgements

This work was supported by the NERC-funded project GR3/ NE/H004963/1 Glacial Activity in Neoproterozoic Svalbard (GAINS). Logistical support was provided by the University Centre in Svalbard. This work was granted access to the HPC resources of CCRT under allocation 2014-017013 made by GENCI (Grand Equipement National de Calcul Intensif). We also thank Didier Paillard and Paul Hoffman for stimulating discussions and valuable insights.

Author contributions

Field data were collected and analyzed by IJF, DIB, EJP, MJH, EAMcM, MSP, PMW and CTES. Geochemical analyses were conducted by HB and PMW. Model experiments were designed and conducted by GLeH, YD, CD and GR. The manuscript and figures were drafted by DIB, IJF and GLeH, with contributions from the other authors.

Competing financial interests

The authors declare no competing financial interests.

Figures:

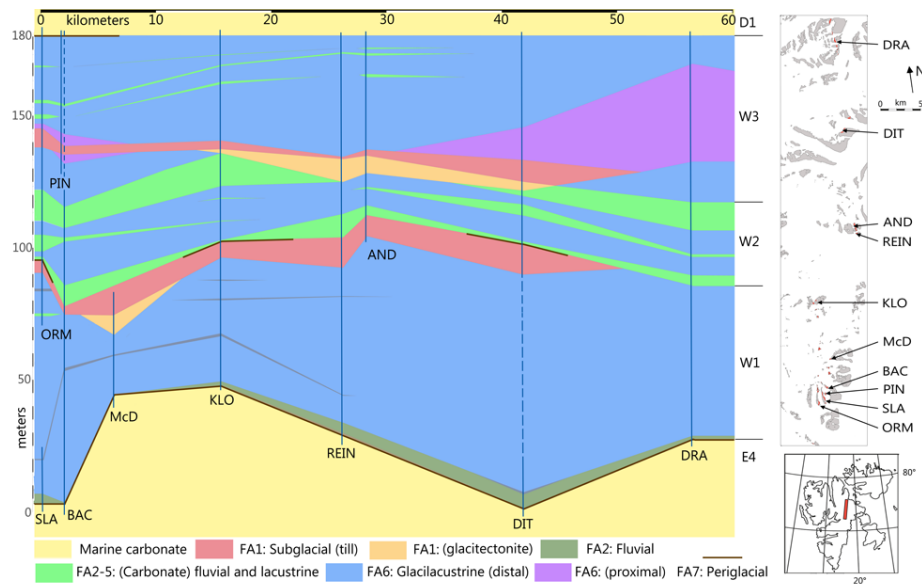


Figure 1: Sedimentary architecture and palaeoenvironments of the Wilsonbreen

Formation. Regional correlation of facies associations and members W1, W2 and W3

across NE Svalbard. From north to south, study locations are: DRA: Dracoisen; DIT:

Ditlovtoppen; AND: East Andromedafjellet; REIN: Reinsryggen (informal name); KLO:

Klofjellet; McD: MacDonaldryggen; BAC: Backlundtoppen - Kvitfjellet ridge; PIN:

Pinnsvinryggen (informal name); SLA: Slangen and ORM: Ormen.

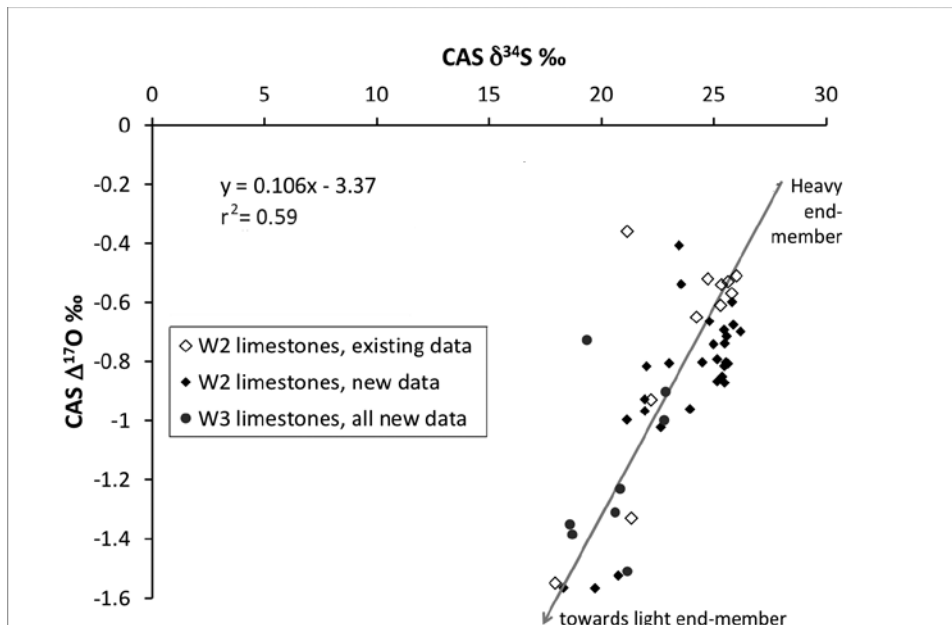


Figure 2: Co-variation of $\Delta^{17}\text{O}$ and $\delta^{34}\text{S}$ from carbonate-associated sulphate in W2 and W3. 'Existing data' (ref. 16) and new data define a mixing line between pre-glacial sulphate (top) and an isotopically light sulphate formed by oxidation of pyrite including incorporation of a light- $\Delta^{17}\text{O}$ signature from a CO_2 -enriched atmosphere. Data from W2 and W3 lie on closely similar trend lines, indicating no detectable change in $p\text{CO}_2$ between deposition of the two members.

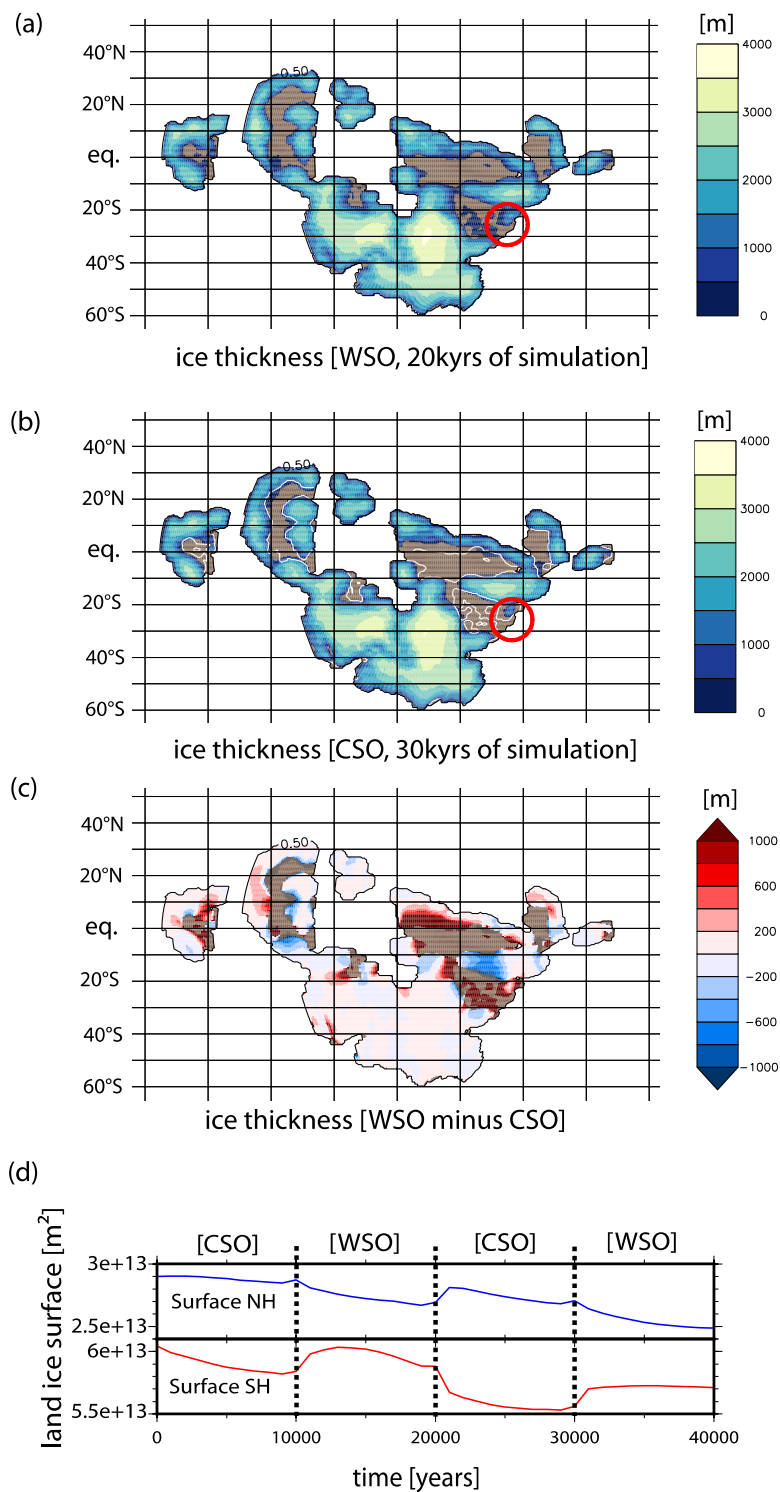


Figure 3: Modelled ice sheet oscillations in response to orbital forcing. (a), (b)

shaded contours show land ice thickness obtained with 20 mbar of carbon dioxide in response to changes of orbital forcing (WSO and CSO, warm/cold summer orbit for the northern hemisphere) over the course of two precession cycles (40 ky of simulation). In light brown continental areas without ice, the white line is used to represent the old ice-sheet extension (WSO case). The Svalbard area is indicated by a red circle. (c) ice thickness variation in 10 ky (WSO case after 20 ky minus CSO case after 30 ky of simulation) (d) surface of hemisphere covered by ice (m^2) through time ([WSO] and [CSO] indicate which orbital configuration is used).